Environmental Pollution 288 (2021) 117697

Contents lists available at ScienceDirect

Environmental Pollution

journal homepage: www.elsevier.com/locate/envpol

Nanoplastics transport to the remote, high-altitude Alps☆

Dušan Materić [a,*], Elke Ludewig [b], Dominik Brunner [c], Thomas Röckmann [a], Rupert Holzinger [a]

[a] Institute for Marine and Atmospheric Research Utrecht, Utrecht University, Princetonplein 5, 3584CC, Utrecht, the Netherlands
[b] ZAMG – Zentralanstalt für Meteorologie und Geodynamik, Sonnblick Observatory, 5020, Salzburg, Freisaalweg 16, Austria
[c] Laboratory for Air Pollution/Environmental Technology, Empa, Swiss Federal Laboratories for Materials Science and Technology, 8600, Dübendorf, Switzerland

ARTICLE INFO

Keywords:
Microplastics
Nanoplastics
Snow
TD-PTR-MS
PTR-MS

ABSTRACT

Plastic materials are increasingly produced worldwide with a total estimated production of >8300 million tonnes to date, of which 60% was discarded. In the environment, plastics fragment into smaller particles, e.g. microplastics (size < 5 mm), and further weathering leads to the formation of functionally different contaminants – nanoplastics (size <1 μm). Nanoplastics are believed to have entirely different physical (e.g. transport), chemical (e.g. functional groups at the surface) and biological (passing the cell membrane, toxicity) properties compared to the micro- and macroplastics, yet, their measurement in the environmental samples is seldom available. Here, we present measurements of nanoplastics mass concentration and calculated the deposition at the pristine high-altitude Alpine Sonnblick observatory (3106 MASL), during the 1.5 month campaigh in late winter 2017. The average nanoplastics concentration was 46.5 ng/mL of melted surface snow. The main polymer types of nanoplastics observed for this site were polypropylene (PP) and polyethylene terephthalate (PET). We measured significantly higher concentrations in the dry sampling periods for PET ($p < 0.002$) but not for PP, which indicates that dry deposition may be the preferential pathway for PET leading to a gradual accumulation on the snow surfaces during dry periods. Air transport modelling indicates regional and long-range transport of nanoplastics, originating preferentially from European urban areas. The mean deposition rate was 42 (+32/-25) kg km^{-2} year^{-1}. Thus more than 2×10^{11} nanoplastics particles are deposited per square meter of surface snow each week of the observed period, even at this remote location, which raises significant toxicological concerns.

1. Introduction

Plastics pollution has been recognised to be a global problem, as particles of various sizes have been detected in water, soil and air, from urban to remote areas (Allenet al., 2019; Dris et al., 2016; Ivleva et al., 2017; Ter Halleet al., 2017). Plastics are one of the most commonly used materials, with an annual production of 359 million tonnes worldwide, of which 61.8 million tonnes (17.2%) are produced in Europe (PlasticsEurope, 2019). It is estimated that >4900 million tonnes of plastics have been disposed in the environment to date (Geyer et al., 2017). There, plastics fragment from bigger to smaller particles, e.g. from macroplastics (>5 mm) to microplastics (size <5 mm), and then further down to nanoplastics (particles <1 μm) (Ivleva et al., 2017; El Hadri et al., 2020; Pradelet al., 2020; Lehner et al., 2019; Mintenig et al., 2018).

Recent studies reported high amounts of microplastics in urban (e.g. London) and remote air (e.g. French Pyrenees, Arctic Fram Strait and protected areas of the USA), and the latter illustrates the important role of long-range transport of airborne microplastics (Allenet al., 2019; Wright et al., 2020; Evangeliouet al., 2020; Bergmannet al., 2019). It has also been shown that microplastics can be transported from air to sea, and very recently, a study showed emission from the sea surface back to air (Allenet al., 2020; Liuet al., 2019). These studies suggest that different environmental systems (sea, land and freshwaters) are interconnected and exchange large amounts of plastics via the air. Furthermore, it has been reported that plastic material exposed to the air fragments more quickly compared to, for example, plastics submerged in seawater (Napper and Thompson, 2019). Accordingly, we can expect a faster degradation of microplastics to nanoplastics in the air (or at the polymer surfaces exposed to the air), and the resulting loads of nanoplastics could be concerning.

The smaller the particles are, the more prominent their toxicological importance becomes (Lehner et al., 2019). Nanoplastics have been reported to cause various adverse effects in studies where organisms or

☆ This paper has been recommended for acceptance by Bernd Nowack.

* Corresponding author.
E-mail address: d.materic@uu.nl (D. Materić).

https://doi.org/10.1016/j.envpol.2021.117697
Received 29 April 2021; Received in revised form 4 June 2021; Accepted 30 June 2021
Available online 9 July 2021

cells have been artificially exposed, usually to a high dosage of polystyrene (Lehner et al., 2019; da Costa et al., 2016; Ferreira et al., 2019). However, data on nanoplastics types and loads that we are exposed to are exceedingly scarce for environmental samples (Mintenig et al., 2018; Schwaferts et al., 2019). Furthermore, most of the current studies focus on the adverse effects that nanoplastics cause in model organisms after *ingesting* a certain amount of polymer. However, there is growing evidence that a significant part of micro- and nanoplastics exposure could enter the body via air *inhalation* (Lehner et al., 2019).

While more data are becoming available on urban and remote microplastics pollution, the concentration of airborne nanoplastics has not been measured yet in the natural environment, primarily due to analytical challenges (Mintenig et al., 2018). We recently developed a chemical method based on Thermal Desorption - Proton Transfer Reaction - Mass Spectrometry (TD-PTR-MS), to selectively quantify nanoplastics of different types with the highest sensitivity reported to date (Materić et al., 2020). In this work, we quantified different types of nanoplastics sampled daily in surface snow at the high-altitude research station Sonnblick Observatory of the ZAMG (Zentralanstalt für Meteorologie und Geodynamik) in the Austrian Alps over the winter-spring transition 2017. The Sonnblick Observatory is located on the peak of the mountain Hoher Sonnblick at 3106 m above sea level. Sonnblick data are regularly used in air quality research and monitoring on regional, continental and global scales (Holzinger et al., 2010; Karlet al., 2001; Kasper and Puxbaum, 1998; Els et al., 2019). Using meteorological data and backward trajectories of air movement, we were able to infer source regions and transport pathways to this remote area.

2. Materials and methods

2.1. Sampling

The samples were taken at a high-altitude, remote site close to the Sonnblick Observatory, Austria (3106 m above sea level), 50 m south from the station building. Daily samples were taken at ~8 a.m. local time (7 a.m. UTC), from 2017 to 02–08 until 2017-03-19 where the surface snow (2 cm depth) was directly sampled (scooped) into 50 mL clean polypropylene vials. This procedure resulted in a volume of 10–25 mL liquid equivalent for each sample (38 samples in total for all the period). We did not take sampling replicates. All the samples were taken at the same location within 1 m distance from each other (the exact location was marked by a tall metal rod). We also took 4 field blanks (distributed throughout the sampling period, see SI), pouring similar amounts of ultrapure water (HPLQ water, VWR International, France) into the same type of vials (polypropylene). Samples and field blanks were kept frozen until analysis.

2.2. Sample preparation and TD-PTR-MS

The samples and field blanks were melted at room temperature, well shaken (not vortexed), and directly filtered with PTFE syringe filters (hand pressure, no wetting agents used), pore size 200 nm into clean glass vials (10 mL, transparent GC-MS vials, VWR International, France). Sample preparation and successive TD-PTR-MS was performed following the detailed methodological protocols defined in our previously published works (Materić et al., 2020; Materić et al., 2019; Materićet al., 2017; Peacock et al., 2018). In short, 1.5 mL of samples/blanks were loaded into new, prebaked (250 °C, overnight) 10 mL chromatography vials and the water was removed in a low-pressure evaporator. Dried samples, field blanks and procedural blanks (HPLQ water loaded in the lab) were thermally desorbed using the following protocol: 3 min incubation at 35 °C, temperature ramp 40 °C/min until 350 °C, then 5 min at 350 °C. The organics coming from the TD were continuously monitored with 1 s time-resolution by PTR-TOF-MS (PTR8000, Ionicon Analytik, Austria) using the protocol described earlier (E/N 120 Td, drift tube temperature 120 °C, Inlet temperature 180 °C).

2.3. Data analysis

TD-PTR-MS data were analysed as described in our previous work (Materić et al., 2020; Materić et al., 2019; Peacock et al., 2018). In short, ion concentrations presented in the data obtained by TD-PTR-MS were extracted using the software package PTRwid (Holzinger, 2015). Final mass spectra were generated by integrating the signal from the point where the TD oven temperature reached 50 °C for the next 10 min of the TD program (mass spectra available in the Supplementary Information). Background subtraction and detection of ions was done according to the procedures developed for ions close to the detection limit (Materićet al., 2017). In short, firstly, we analysed the total volume of each sample (divided into 1.5 mL loads); secondly, we generated average mass spectra for each sample representing 1.5 mL sample load; and finally, we applied subtraction (using the mean of the blanks) and detection limit filtration (3σ of the blanks) based on 1.5 mL sample load. The resulting mass spectra were converted to concentration information (in ppb) for each organic ion, which was calculated according to the formula:

$$C = \frac{1}{kt} \times \frac{[M{\cdot}H^+]}{[H_3O^+]} \times \frac{\sqrt{(m/z)_{H_3O^+}}}{\sqrt{(m/z)_{M{\cdot}H^+}}}$$

where C is concentration, k is reaction rate coefficient, t the residence time of the primary ions in the drift tube, $[M{\cdot}H^+]$ and $[H_3O^+]$ are ion counts representing the protonated analyte and primary ions, respectively, $(m/z)_{H3O+}$ and $(m/z)_{M{\cdot}H+}$ represent mass-to-charge ratio of protonated water and the protonated analyte *M,* respectively. This concentration calculation is possible based on the extensive knowledge of proton transfer reactions that occur in the instrument chamber, and it is generally accepted with the uncertainty of ± 30% (Materićet al., 2017; Peacock et al., 2018; Cappellinet al., 2012; Lindinger et al., 1998; Holzingeret al., 2019). Results from a recent intercomparison campaign of 11 PTR-MS instruments (Holzingeret al., 2019) suggest that if the PTR-MS transmission is known through calibration with multi-trace standards (i.e., standards containing known traces covering the relevant time-of-flight span of the instrument), such as in our case, the uncertainty is even ~10%. However, we took a more conservative approach and reported 30% uncertainty for all of our measurement.

Nanoplastics fingerprinting and quantification was performed as described earlier in (Materić et al., 2020). We used 40 unique ions from the mass spectra of virgin plastics (each plastic type separately) and performed fingerprinting over the mass spectra of the snow samples. The similarity between the library mass spectra and samples mass spectra was scored (Materić et al., 2020) and, if above the calculated threshold, the fingerprint was set as positive (for the details refer to our previous work (Materić et al., 2020)). The threshold score was calculated based on 1000 random/synthetic mass spectra, which included the same 40 ions as in the library mass spectra. If the signal was 2σ above the average of the synthetic spectra (z-score = 2, $p < 0.02275$, one tail distribution, e.g. score 47.8 or 32.7 for the algorithm 1 and 3 respectively, for PET), we assigned a positive fingerprint. Many positive fingerprints in our sample were 3σ ($p < 0.00135$) or more above the calculated synthetic spectra (see the Supplementary Information).

2.4. Deposition calculation

The snow surface is a dynamic system where deposition and loss of the nanoplastics particles, and other analytes, happen simultaneously (Materić et al., 2019). In the case of no precipitation, the snow surface is exposed to the air and over time the concentration of the analyte increases due to dry deposition (assuming no losses). In this work, we took a conservative approach and did not compensate for possible losses. Thus, the dry deposition rate *(D)* is calculated from the difference

between concentrations *(C)* measured at two different times (days).

$$D = C_{day\ x} - C_{day\ x-1}$$

During precipitation days, the concentration of nanoplastics measured in new snow was entirely attributed to wet deposition (without correcting for the precipitation column).

The deposition per surface area was calculated assuming on average 2 cm sampling depth (±0.5 cm) and a snow density of 250 mg/mL (±100 mg/mL). That way we calculated that 1 cm^2 of snow surface on average corresponds to 0.5 mL of melted snow (+75%, −60% - the uncertainties are calculated using the above-mentioned maximum deviations of the sampling depth and snow density).

The deposition loads reported here are not correct for any losses (e.g. losses of neutral molecules during proton transfer reaction (Materić et al., 2020), losses at the snow surface due to the wind, see Appendix Fig. A.4). The processes at the snow surface, such as sublimation and "scrubbing effect" of the snow, might to some extent enrich the initial concentration of nanoplastics and, in turn, affect our deposition estimation. Furthermore, nanoplastics might come to the site and deposit as much larger particles, e.g. hetero-aggregates (Oriekhova and Stoll, 2018), and might also dynamically form from already aged microplastics. Thus, the deposition values we report here might have large uncertainty.

Regarding the number concentration, we assumed that all nanoplastics particles have the maximum possible size of the filter mesh (200 nm). The real number concentration is likely much larger as the number of particles exponentially grow as the particle sizes decrease, and the filter mesh could retain some particles smaller <200 nm.

2.5. HYSPLIT model

The HYSPLIT dispersion model (Steinet al., 2015) was used to track the particles 96 h h backwards, considering a particle size of 0.2 μm (cut-off size of our filtering), a density of 1 g/cm^3, spherical shape and no deposition forced. We noticed no impact on the resulting footprint when nanoplastics were modelled as gas or as particles of 0.2 μm diameter, since gravitational settling is negligible for such small particles. Footprints also did not differ between simulations without and with deposition (e.g. deposition velocities of 0.034 cm s^{-1}) (Duan et al., 1988; Gallagheret al., 2002). The sampling location was at the top of the mountain (3106 m above sea level), and the HYSPLIT model does not accurately calculate altitude but rather uses the average altitude of the topography at the resolution of the grid. To compensate for this, we started the trajectories at the pressure level corresponding to the pressure measured at the Sonnblick Observatory (where the samples were taken) at the sampling time. Particles were released at Sonnblick over 24 h (corresponding to frequency of the daily samples) and then followed backward in time over 72 more hours. The total time of a simulation was thus 96 h. The resulting source footprint area is the area where the dispersed particles were in contact with the surface (<100 m above ground level, a default set up (Steinet al., 2015)). To investigate the influence of human activity, we weighted the surface contact with population density from GEOSTAT (T - Eurostat (Novem, 2020). The frequency map for the entire period was calculated based on the 96 h HYSPLIT backward trajectories. The model outputs are available in the Supplementary Information.

2.6. Statistics

Differences were examined for significance using *t*-test (two groups/levels) or and one-way ANOVA (more than two groups/levels). In both cases, we used a two-tailed distribution, and n-1 degrees of freedom (where n is the number of groups/levels). After one-way ANOVA, to determine where the significance exist, we used Tukey's test (95% family-wise confidence level), and p-values are reported in the figures.

2.7. Quality assurance

Contamination of nanoplastics coming from the air is virtually impossible to avoid in the analytical procedure. It is also currently not possible to completely avoid the plastics material used as the labware. Accordingly, great care was taken to evaluate possible contamination. To do so, we took field blanks throughout the monitoring period (4 in total) which were exposed to the same conditions and possible contaminations as the surface snow samples and underwent the same sample preparation procedures. The same personnel of the station took the samples throughout the period in order to make the contamination level constant. We regularly cleaned the lab and working space and avoided movement in the lab (e.g. walking) while handling the open samples (e.g. loading).

Our analysis showed no measurable plastics traces in any of our field blanks when tested for PE, PET, PP, PS and PVC. However, we detected traces of polypropylene carbonate (PPC) in some field blanks 6.3 ng/mL (ranging 0–15.2 ng/mL, see Supplementary Information), likely coming from our labware. The sampling protocol for this experiment was initially designed to characterise dissolved organic matter in the snow (e.g. organic aerosols) (Materić et al., 2019; Materićet al., 2017), and 50 mL PP containers were used. The samples and blanks were stored in these containers for several months until analysis. However, we did not detect any PP in any of the field blanks (the PP container material was used to create a PP spectra for the library).

The mass spectrometric fingerprints of PP and PPC are not sufficiently different to clearly separate these plastics in natural samples that contain natural dissolved organic matter (Materić et al., 2020). In this work, we refer them as PP following the negligible production/use rate of PPC compared to PP (PlasticsEurope, 2019). Possible contamination of our PP/PPC measurements was corrected in our data processing by means of blank subtraction.

Given the detection limit of the technique (0.2 ng in a sample) (Materić et al., 2020), and our sample loads of 1.5 mL, we calculated that if any contamination of PE, PET and PS occurred in our experiment, it was below 0.13 ng/mL (0.2 [ng]/1.5 [mL]).

In addition to the previously published quality assessment of our method (considering potential false-positive and false-negative fingerprints due to the presence of natural dissolved organic matter) (Materić et al., 2020) we performed additional experiments to exclude artefacts. 1) We ran an experiment with common natural polymers (cellulose and humic acids) to experimentally test their potential to produce false-positive attributions. We conclude that there is no positive match between these polymers and any of the plastics we analysed (PE, PET, PS, PP, PPC, PVC, Tire wear) (see the SI). 2) To test for potential false-negatives, we spiked mix of natural polymers (cellulose and humic acids) with 100 ng of PS. Our fingerprint match was positive, concluding that the presence of these common natural polymers does not significantly disturb the fingerprint performance (see the SI). The measured mass of PS in these spiked samples by TD-PTR-MS was 9.2 ± 1.2 ng, which is in the expected range reported earlier for semi-quantitative measurements (e.g. neutral molecules formed in the PTR, molecule fragments, CH_4 and CO_2 are not visible by PTR-MS) (Materić et al., 2020).

3. Results

3.1. Nanoplastics concentrations

Measured nanoplastics concentrations in surface snow samples in the period 2017-02-08 until 2017-03-19 (38 daily measurement points) are presented in Fig. 1 together with meteorological conditions (detailed meteorological conditions in Appendix Fig. A.1, Table A.1). The nanoplastics concentrations are retrieved using the TD-PTR-MS method published earlier, utilising the mass spectrometric fingerprints for each plastics type (e.g. see Appendix Fig. A.2) (Materić et al., 2020;

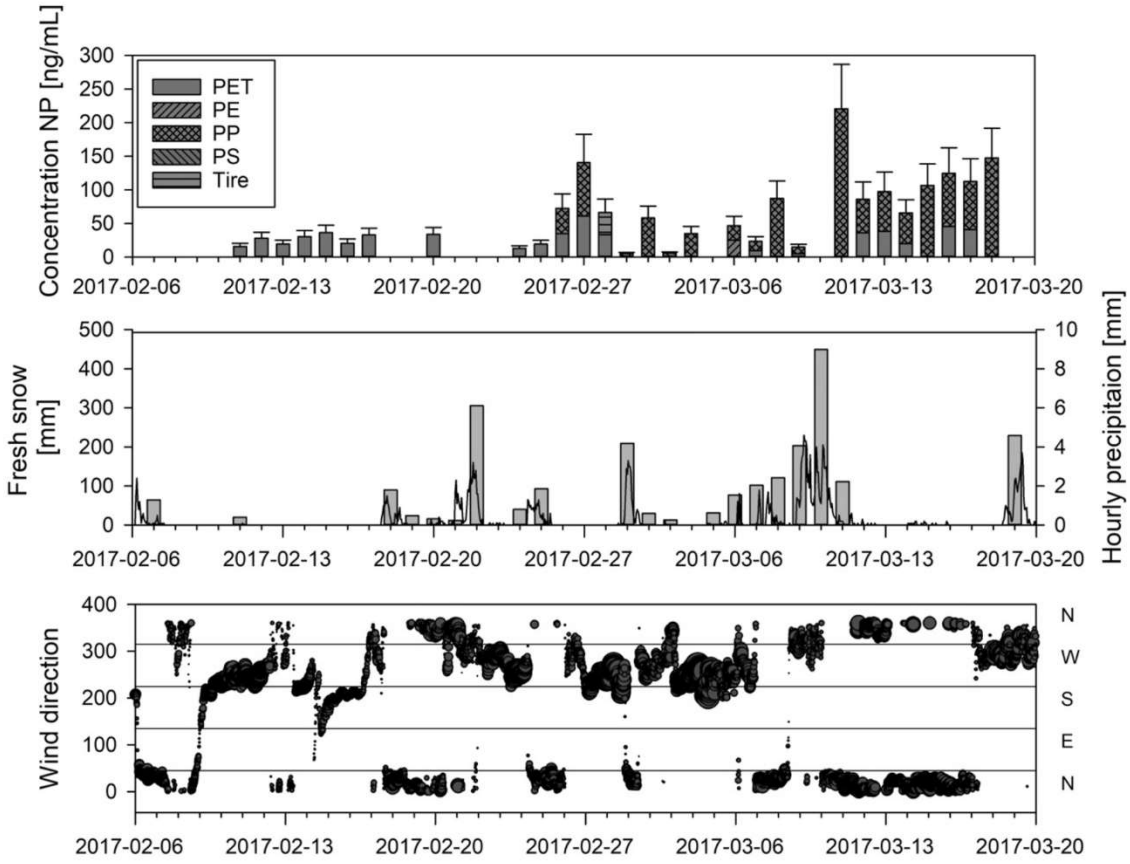

Fig. 1. Concentrations of nanoplastics (NP) in high-altitude surface snow and associated meteorological conditions for the site. PET – polyethylene terephthalate, PE – polyethylene (2017-03-06), PP – polypropylene, PS – polystyrene, (2017-03-01 and 2017-03-03), Tire – tire wear (2017-02-28). Uncertainty bars represent general PTR-MS quantification associated uncertainty of 30% (see method section for details) (Cappellinet al., 2012; Holzingeret al., 2019). Daily fresh snow precipitation in mm represents 24 h precipitation prior to the sampling time (~7:00 UTC). Maximum 10 min average wind comes from S and SW, 26 m/s (SI Appendix Table SI1). For detailed meteorological conditions, see SI Appendix Fig. SI1.

Materićet al., 2017; Peacock et al., 2018). The mass spectral library we use contains standard polymers that have no additives. This way, we aimed to fingerprint only the ion products of the plastics polymer and minimize the potential impact of different additives or degradation stages expected in nature on the analysis.

We note that chemical ionization of thermally desorbed plastics vapours also generates neutral molecules (e.g. CO_2) that are not seen by the method, thus the concentrations we report are conservative and represent lower limits (for details see the methods section and our previous publication (Materić et al., 2020)).

Over the study period, the mean nanoplastics concentration in the surface snow was 46.5 ng/mL, the predominant detected plastics types were polyethylene terephthalate (PET) and polypropylene (PP) with mean concentrations of 15.1 and 29.5 ng/mL of melted snow, respectively. Both plastics belong to the most used non-fibre plastic materials, contributing up to 7.7% and 19.3% to the European demand (PET and PP respectively) and, PET accounts for 70% of synthetic fibre production (PlasticsEurope, 2019; Geyer et al., 2017). The PP contribution that we measured was increasing towards the end of the period (Fig. 1), together with the concentrations of other organics (e.g. dissolved organic matter signatures detectable with TD-PTR-MS) (Appendix Table A.2). In this period, besides PP and PET, we occasionally also measured small amounts of polyethylene (PE) and polystyrene (PS), 25 and 5 ng/mL respectively. This increase in the nanoplastics concentration and variety over the monitoring period agrees with the previously observed seasonal change of fine particle deposition at the site due to seasonal variations in the efficiency of upward transport of air from the planetary boundary layer (e.g. notably lower deposition rates from October to February, compared to the rest of the year) (Kasper and Puxbaum, 1998).

We compared the nanoplastics concentrations to the total organics retrieved with TD-PTR-MS (<200 nm) and noted that nanoplastics contribute on average 14.2% (range 6.6–44.5%) to the organics measured by the method (Appendix Table A.2). Since the TD-PTR-MS technique is only selective to low molecular weight organic matter (<500 Da) covering on average 5.5% (0.4–11.8%) of natural dissolved organic matter (Peacock et al., 2018), this translates into an average of 0.8% (0.3–2.4%) of dissolved organic matter present in the surface snow consisting of nanoplastics colloids <200 nm.

3.2. Dry and wet deposition of nanoplastics

We further explore the correlations between nanoplastics deposition and precipitation events in order to understand which types of nanoplastics are preferentially delivered to the site as a dry or wet deposition. During the measurements period, we had 20 wet and 21 dry days. We measured significantly higher concentrations in the dry sampling periods for PET (Fig. 2, $p < 0.002$), but not for PP. Thus, dry deposition may be the preferential pathway for PET leading to a gradual accumulation on the snow surfaces during dry periods. The importance of dry deposition for small nanoplastics would provide a mechanistic explanation for the observation in protected areas of the US where dry periods typically had microplastics particles smaller in size compared to the wet period (Brahney et al., 2020). However, measured PP concentrations, which are not correlated with precipitation levels, suggest that different deposition mechanisms may apply for different nanoplastics types.

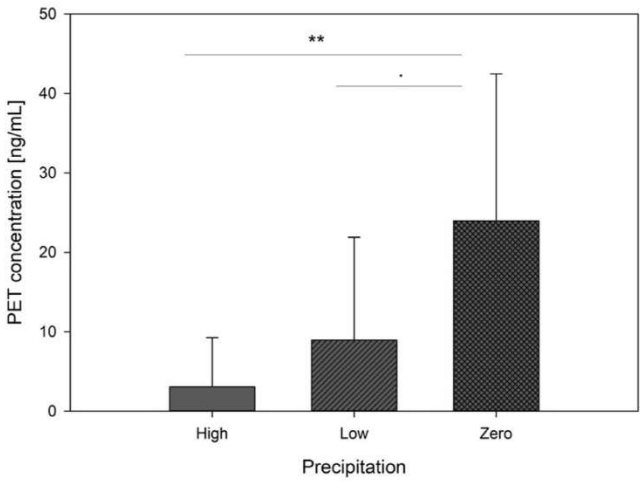

Fig. 2. Comparison between nanoplastics concentrations and snow precipitation levels (High >50 mm/day, Low >0 and < 50 mm/day and Zero – no precipitation). Symbols "**" and "." represent significant difference of $p < 0.002$, $p < 0.072$, respectively (one-way ANOVA analysis of variances, *F*-value = 7.62) between the bars linked by the line. Error bars are SD of measurements in each precipitation group (n = 5, 7 and 20 for High, Low and Zero, respectively).

3.3. Nanoplastics deposition rates and upscaling

Weekly deposition rates of different types of nanoplastics are shown in Fig. 3a, where on average we measured nanoplastics deposition of 167.6 ng/mL week^{-1}, albeit with huge variability (range: 28–429 ng/mL week^{-1}). Considering that according to our sampling protocol 1 mL of snow corresponds to roughly 2 cm^2 of snow surface (25), we calculate a mean deposition rate of 800 μg m^{-2} week^{-1} (uncertainties +608 and −486 μg m^{-2} week^{-1}). This translates to a yearly deposition of 43.7 (+32.8/-26.2) kg of nanoplastics per km^2. We measured the nanoplastics after filtering the water with a 200 nm pore size filter. If we assume that all the nanoplastics particles in the sample are spherical particles of 200 nm diameter and density ~1 g/cm^3, 1 ng of nanoplastics consists of 4×10^5 200 nm particles. This, translates to a minimum deposition rate of 200 billion (2×10^{11}) nanoplastics particles per square meter per week (Fig. 3a).

For comparison, the deposition rate of microplastics in remote protected areas of the US (Brahney et al., 2020) was estimated as 4.2 kg per km^2 per year and 2.8 times higher in the French Pyrenees (only the number of microplastics particles was reported, 336 per m^2 per day) (Allenet al., 2019). This might indicate that the mass concentration of nanoplastics in the air may be 3–10 times higher than what was reported previously for microplastics. However, Bergmannet al., 2019 reported microplastics number concentration in surface snow/ice on average ~1760 and ~700 MP per L in Arctic and Alps (Bergmannet al., 2019). Note these are number concentration values. If we assume MPs size of 11 μm (the detection limit for FTIR), the density of 1 g/cm^3 and spherical shape, we calculate the mass concentration of 1672 and 665 μg/L in snow from the Arctic and Alps, respectively. These concentrations of MPs are order(s) of magnitude higher than what we measured for NPs <200 nm (on average 46.5 μg/L). Apparently, there is a large MPs concentration difference, possibly site-specific and related to the sampling strategies.

4. Discussion

4.1. Atmospheric transport of nanoplastics

It is not surprising that airborne transport of nanoplastics is much more effective than for microplastics, because lighter particles can be transported over longer distances from the sources. Also, plastics extensively fragment when exposed to the air (Napper and Thompson, 2019), which implies that open-air exposure of plastics surfaces, e.g. microplastics fibres from clothing (mostly PET), can lead to the formation of nanoplastics during atmospheric transport. This might be a significant contributor to the overall PET burden we observed throughout the measurement period. Furthermore, nanoplastics might come to the site and deposit as hetero-aggregates (e.g. with organic matter and black carbon) (Oriekhova and Stoll, 2018; Dubaish and Liebezeit, 2013) and might also dynamically form from already aged microplastics after deposition.

Linking the temporal evolution of our measurements to air mass transport elucidates potential sources and pathways of nanoplastics transport to the observatory. Accordingly, we used the HYSPLIT dispersion model (Steinet al., 2015) to calculate source footprints for surface contact of the air parcel, and footprints weighted by population density (Fig. 3c, for the model setup, see methods). We found that the deposition rate of the nanoplastics strongly correlates ($r^2 = 0.8293$, p-value = 0.0036) with the population weighted footprint classes (Fig. 3b). Although nanoplastics deposition is a complex process involving a mix of potential local, regional and global sources, our data provide evidence that densely populated urban areas might be hotspots of nanoplastics emission. For example, on 2017-03-11 we recorded the single highest nanoplastics concentration of >200 ng/mL, and the associated footprints indicate a major contribution from populated areas in England, France, the Netherlands and Germany, including the major cities: London, Paris, Amsterdam, Frankfurt, Stuttgart and Munich (Fig. 3c).

However, our data also suggest that some deposition could come from a long distance, beyond the European continent. On 2017-02-15, we measured a deposition rate of 6 ng/mL, but the vertical profile of particle dispersion suggests that the air stayed at high altitudes above Europe and had no contact to the surface. The last surface contact was 96 h backwards, above the Atlantic Ocean – more than 3000 km away from the site (Appendix Fig. A3, Appendix Table A.2). These nanoplastics may originate from sources that are even further away and are (at least sometimes) present at significant concentrations at high-altitudes in the free troposphere above continental Europe. Marine sources have been suggested as significant contributor to atmospheric microplastics (Allenet al., 2020), which may be another process explaining the nanoplastics deposition we measured for this date.

The footprint analysis presented in Fig. 3d illustrates the origin of the air reaching the Sonnblick Observatory during the entire monitoring period. Most of the trajectories (>30%) indicate a potential particle origin from densely populated, nearby European areas that are 200 km away from the site (Southern Germany, Northern Italy, Switzerland, Eastern France and Slovenia). The trajectories also suggest possible long-range and global transport of nanoplastics, with 10% of the trajectories originating from more than 2000 km away (Fig. 3d). This is consistent with the previously observed reported atmospheric transport and potential source analysis for other fine particles (aerosol, microorganisms) monitored at the station (Holzinger et al., 2010; Karlet al., 2001; Kasper and Puxbaum, 1998; Els et al., 2019).

5. Conclusions

Our detection of nanoplastics in the remote Alps together with previously published measurements of microplastics in remote areas demonstrate global scale atmospheric pollution with these emerging contaminants. The total nanoplastics mass deposition we estimate in this study might be similar to previously published atmospheric microplastic deposition in remote areas (Brahney et al., 2020). Considering the potentially greater toxicological importance, it is crucial that further research in the field focuses on atmospheric nanoplastics pollution. It is well established that aerosol pollution significantly affects human health, decreasing life expectancy up to 5 years in urban areas (Apte

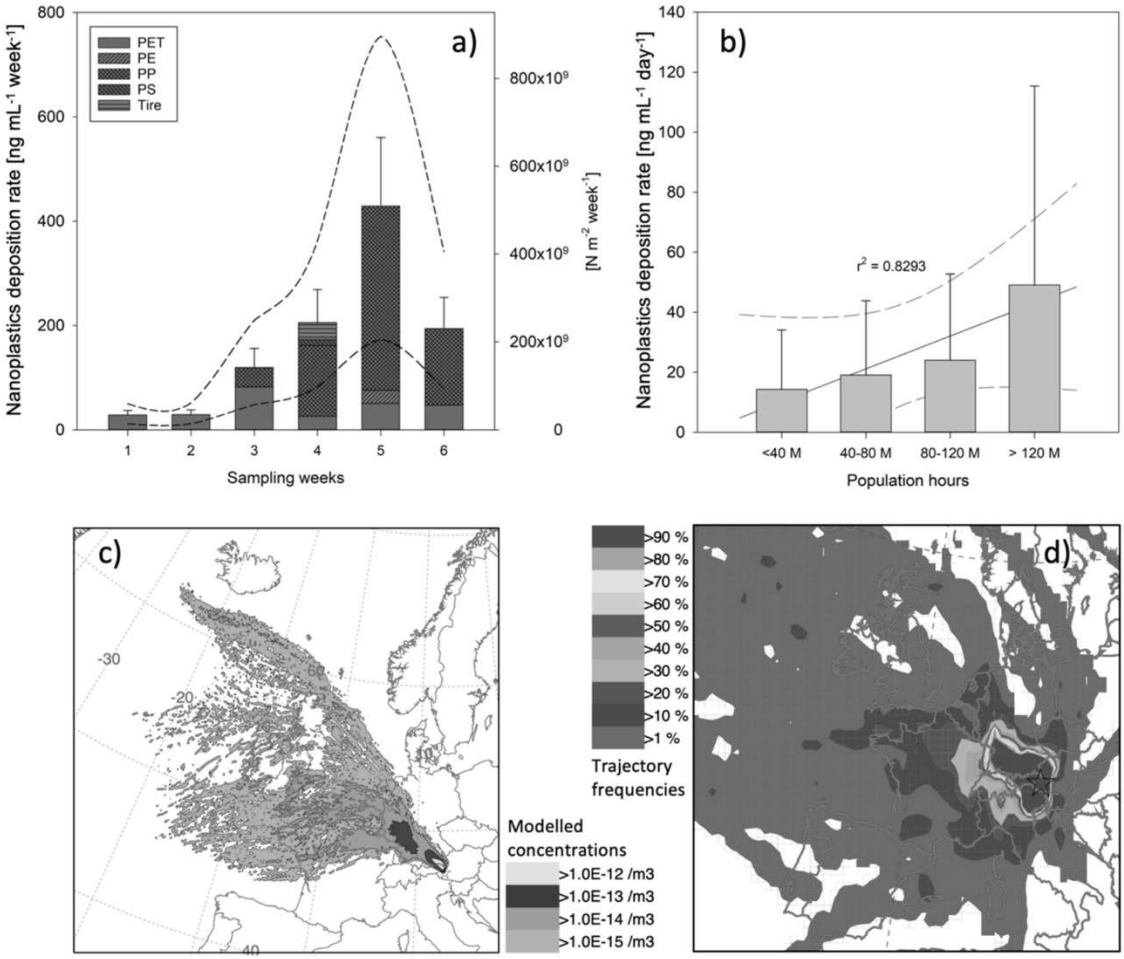

Fig. 3. Deposition of nanoplastics at the Sonnblick Observatory, Austria (3016 m above sea level); source dependent deposition rates and trajectories. A) Weekly mass and lower limit of number deposition rate of the nanoplastics. Error bars represent general PTR-MS uncertainty of 30% associated with quantification (Cappellinet al., 2012; Holzingeret al., 2019). Dashed lines represent estimated uncertainty ranges (+75 and −60%) associated with sampling conditions (e.g. changes in snow density, see the Method section). B) Nanoplastics deposition rate as a function of the population exposure. Error bars represent the standard deviation of measurements in each population group (n = 9, 14, 5 and 10 for <40, 40–80, 80–120 and > 120 million people hours, respectively). *p*-value = 0.0036. C) Source areas (footprint) calculated with HYSPLIT backward dispersion simulations for air arriving at Sonnblick on 2017-03-11, representing the single highest nanoplastics concentration observed (>200 ng/mL). D) HYSPLIT source areas averaged over the whole sampling period, ranging as far as 2000 km with >10% frequency.

et al., 2015). The size of aerosols plays an important role for their toxicity. Small particles of size <1 μm can penetrate deep into the lungs, but larger particles >10 μm are likely filtered out by the upper respiratory system (Oberdörster, 1993). Thus, nanoplastics can penetrate deep in the lungs (alveoli) and given their small diameter can even pass the cell membrane barrier and enter the bloodstream (Lehner et al., 2019; Oberdörster, 1993; Stapleton, 2019; Wright and Kelly, 2017; Revel et al., 2018). Further measurements of nanoplastics in urban, rural and remote areas are essential to assess the extent of nanoplastics pollution. This will provide insight into the levels of human exposure so that accurate air-quality protocols, toxicological assessment and mitigation efforts can be established.

Data and code availability

The authors confirm that the data and codes underling the results of this publication are available in the Supplementary Information and can be downloaded in conjunction with this paper.

Supplementary information contains: Dataset (Mass spectra of the samples, Fingerprint code with plastics mass spectra library, fingerprint match score reports, meteorological data, trajectory elements).

Raw, unformatted, mass spectra encoded in *.h5* format are available from the corresponding author upon reasonable request.

Author contributions

DM designed the experiment with the help of RH and carried them out. EL provided the samples and meteorological data. DM prepared the paper with contributions from all co-authors.

Declaration of competing interest

The authors declare that they have no known competing financial interests or personal relationships that could have appeared to influence the work reported in this paper.

Acknowledgements

We acknowledge the support from the Netherlands Earth System Science Centre (NESSC) research network and by the Dutch NWO Earth and Life Science (ALW), project 824.14.002, and NWO Domain Science (ENW) project OCENW.XS.06. We thank the operators at the Sonnblick

Observatory of the ZAMG (Zentralanstalt für Meteorologie und Geodynamik) for taking the samples. We thank a student Arno van den Berg for participating in some PTRdom analysis.

Appendix

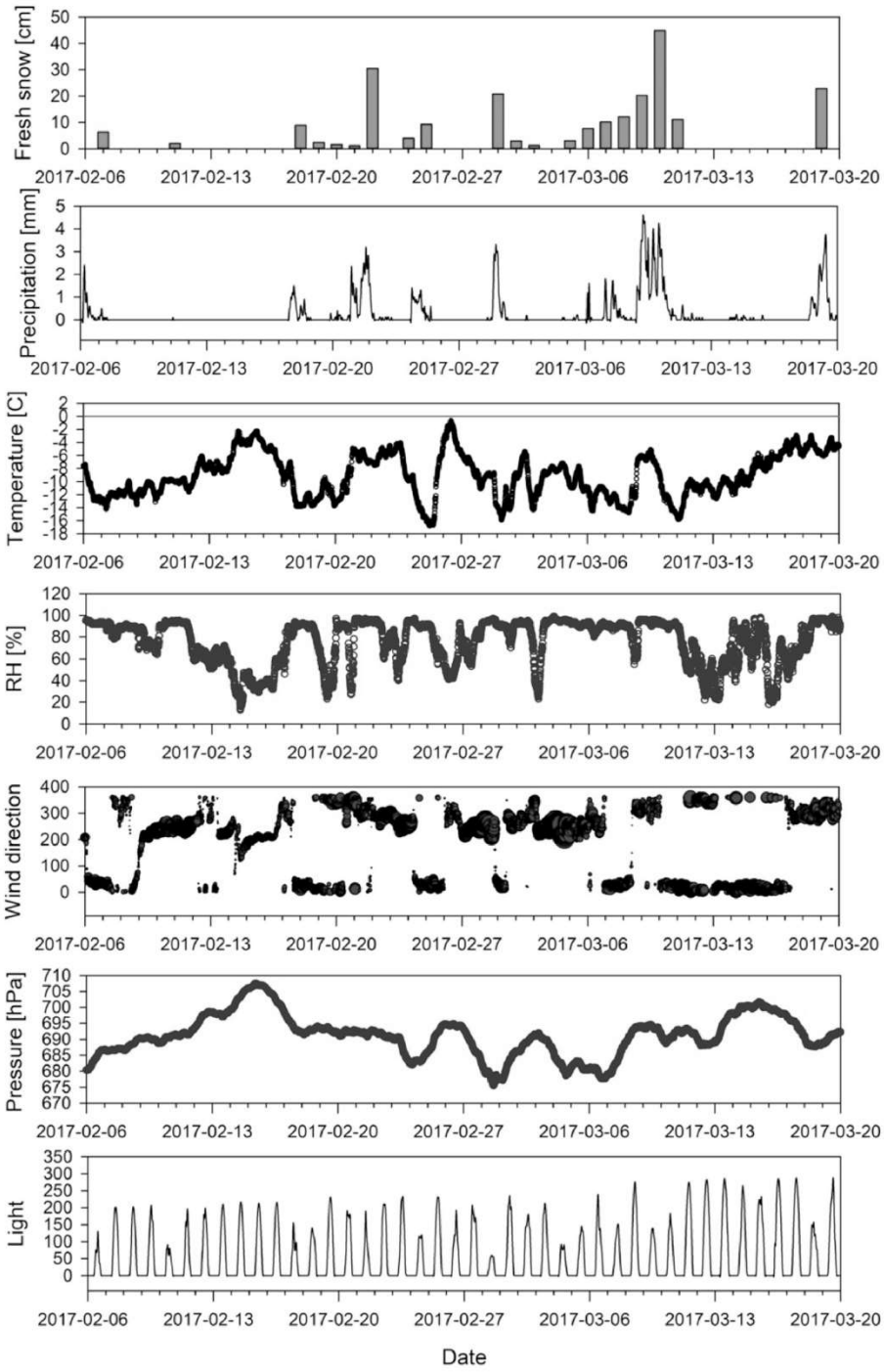

Fig. A.1. Meteorological conditions for the entire sampling period. Daily fresh snow in cm, hourly precipitation in mm, the temperature in °C, Relative humidity in %, wind direction, pressure in hPa and light intensity in W/m^2.

Table A.1
Average daily wind direction and speed for the sampling period. The average was taken 24h back from the sampling time (7.00 UCT).

Date	Average direction [deg]	Average direction	Average speed [m/s]	Maximum speed [m/s]	Fresh snow [cm] – 7-7 AM UCT
2017-02-07	35.2	NE	10.4	13.2	6.4
2017-02-08	218.9	W	4.9	11	0
2017-02-09	157.3	NE	5.0	8.6	0
2017-02-10	226.9	SW	11.7	18.9	0
2017-02-11	248.2	SW	12.9	17.9	2
2017-02-12	251.2	SW	12.9	17.2	0
2017-02-13	186.3	W	3.4	7	0
2017-02-14	217.2	SW	8.9	13.1	0
2017-02-15	172.7	S	5.2	10.1	0
2017-02-16	206.5	SW	7.5	9.3	0
2017-02-17	252.7	W	5.5	8.8	0
2017-02-18	103.9	NE	7.2	14.4	9
2017-02-19	57.9	NE	7.2	9.8	2.4
2017-02-20	231.5	W	8.2	15.3	1.6
2017-02-21	289.6	W	9.0	18.9	1.2
2017-02-22	273.9	W	6.4	14	30.5
2017-02-23	284.6	W	12.2	18	0
2017-02-24	257.5	W	14.3	21.6	4
2017-02-25	39.8	NE	8.2	13.6	9.3
2017-02-26	108.3	NE	6.0	12.5	0
2017-02-27	265.8	W	7.4	13.9	0
2017-02-28	245.4	SW	16.6	21.5	0
2017-03-01	152.5	NE	12.6	22.8	20.9
2017-03-02	219.8	W	9.4	14.5	3
2017-03-03	284.0	W	7.2	14.1	1.3
2017-03-04	244.3	SW	19.1	25.5	0
2017-03-05	241.4	W	16.8	26	3.1
2017-03-06	243.7	SW	8.8	13.8	7.7
2017-03-07	173.1	W	9.0	13.8	10.2
2017-03-08	27.4	NE	9.4	12.9	12.1
2017-03-09	268.5	W	6.8	14.1	20.3
2017-03-10	216.3	W	5.4	10.6	44.9
2017-03-11	25.2	NE	9.6	15	11.1
2017-03-12	128.7	NE	11.2	15.1	0
2017-03-13	222.4	W	9.5	12.8	0
2017-03-14	25.5	NE	8.7	15.2	0
2017-03-15	22.7	NE	12.5	15.8	0
2017-03-16	54.8	NE	11.3	15.3	0
2017-03-17	82.5	NE	6.5	11.6	0
2017-03-18	292.6	W	10.0	20.7	0
2017-03-19	299.5	W	10.1	19.7	22.9

Table A.2
Time-resolved summary of measured nanoplastics (NPs) concentrations, depositions and its contribution to the bulk dissolved organic matter.

Date	Nanoplastics concentration [ng/mL]				Nanoplastics deposition [ng/(mL day)]	PTRdom [ng/mL]	NPs in PTRdom [%]	Modelled NPs in DOM [%]
	PET	PE	PP	PS				
2017-02-08	0.0	0.0	0.0	0.0	0.0	59.5	0.0	0.0
2017-02-10	0.0	0.0	0.0	0.0	0.0	144.9	0.0	0.0
2017-02-11	15.7	0.0	0.0	0.0	15.7	74.5	21.1	1.2
2017-02-12	28.3	0.0	0.0	0.0	12.6	163.4	17.3	1.0
2017-02-13	19.5	0.0	0.0	0.0	0.0	125.8	15.5	0.9
2017-02-14	30.4	0.0	0.0	0.0	11.0	181.9	16.7	0.9
2017-02-15	36.3	0.0	0.0	0.0	5.9	222.8	16.3	0.9
2017-02-16	20.7	0.0	0.0	0.0	0.0	174.3	11.9	0.7
2017-02-17	33.1	0.0	0.0	0.0	12.4	183.5	18.0	1.0
2017-02-18	0.0	0.0	0.0	0.0	0.0	30.6	0.0	0.0
2017-02-20	33.9	0.0	0.0	0.0	33.9	181.4	18.7	1.0
2017-02-21	0.0	0.0	0.0	0.0	0.0	94.1	0.0	0.0
2017-02-22	0.0	0.0	0.0	0.0	0.0	19.3	0.0	0.0
2017-02-23	0.0	0.0	0.0	0.0	0.0	5.4	0.0	0.0
2017-02-24	13.0	0.0	0.0	0.0	13.0	63.8	20.4	1.1
2017-02-25	19.3	0.0	0.0	0.0	19.3	92.9	20.8	1.1
2017-02-26	35.1	0.0	37.4	0.0	53.1	334.1	21.7	1.2
2017-02-27	61.1	0.0	79.4	0.0	68.0	517.8	27.1	1.5
2017-02-28	33.5	0.0	0.0	0.0	0.0	282.0	11.9	0.7
2017-03-01	0.0	0.0	0.0	5.4	5.4	128.8	0.0	0.0
2017-03-02	0.0	0.0	58.3	0.0	58.3	922.6	6.3	0.3
2017-03-03	0.0	0.0	0.0	5.9	5.9	82.9	0.0	0.0
2017-03-04	0.0	0.0	35.1	0.0	35.1	142.7	24.6	1.4

(continued on next page)

Table A.2 (*continued*)

Date	Nanoplastics concentration [ng/mL]				Nanoplastics deposition [ng/(mL day)]	PTRdom [ng/mL]	NPs in PTRdom [%]	Modelled NPs in DOM [%]
	PET	PE	PP	PS				
2017-03-05	0.0	0.0	0.0	0.0	0.0	132.0	0.0	0.0
2017-03-06	0.0	25.2	21.6	0.0	46.8	119.7	39.1	2.2
2017-03-07	9.5	0.0	14.0	0.0	23.5	52.7	44.5	2.4
2017-03-08	0.0	0.0	87.1	0.0	87.1	951.7	9.2	0.5
2017-03-09	4.8	0.0	9.9	0.0	14.7	91.8	16.0	0.9
2017-03-10	0.0	0.0	0.0	0.0	0.0	33540.0	0.0	0.0
2017-03-11	0.0	0.0	220.5	0.0	220.5	2252.4	9.8	0.5
2017-03-12	36.2	0.0	49.9	0.0	36.2	305.9	28.1	1.5
2017-03-13	38.1	0.0	59.3	0.0	11.3	469.1	20.8	1.1
2017-03-14	20.4	0.0	45.4	0.0	0.0	257.7	25.5	1.4
2017-03-15	0.0	0.0	106.6	0.0	61.2	616.0	17.3	1.0
2017-03-16	45.6	0.0	79.3	0.0	45.6	498.9	25.0	1.4
2017-03-17	41.2	0.0	71.4	0.0	0.0	513.7	21.9	1.2
2017-03-18	0.0	0.0	147.4	0.0	76.0	831.4	17.7	1.0
2017-03-19	0.0	0.0	0.0	0.0	0.0	117.6	0.0	0.0
							Average	
Total	575.7	25.2	1122.5	11.3	972.6	44979.6	14.3	0.8

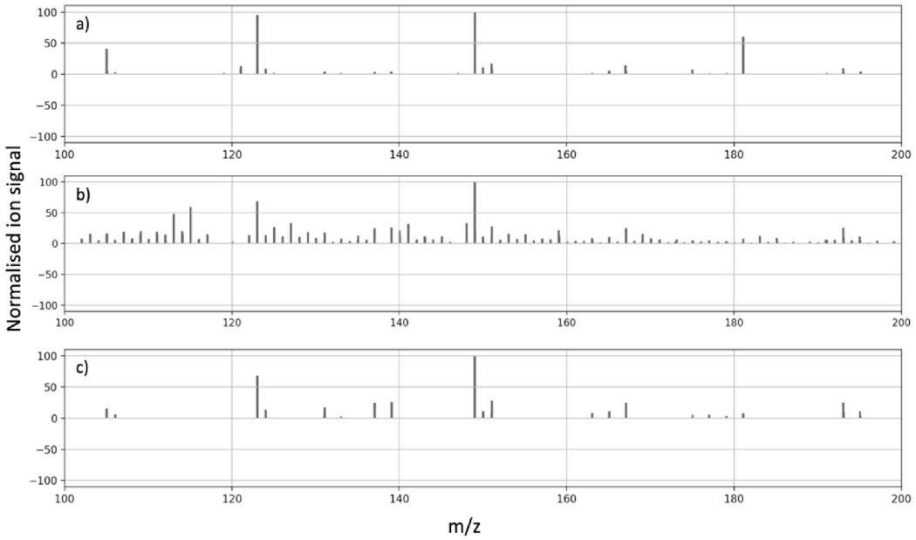

Fig. A.2. Fingerprinting PET nanoplastics in a sample (match confidence '***', z-score > 4), a) Ions in PET library, b) Mass spectra of the surface snow sample (2017-02-28), c) PET nanoplastics signal in the sample (2017-02-28). The signals are normalised to the highest peak. The fingerprint algorithm, scoring and evaluation were in details addressed in our previous work (Materić et al., 2020).

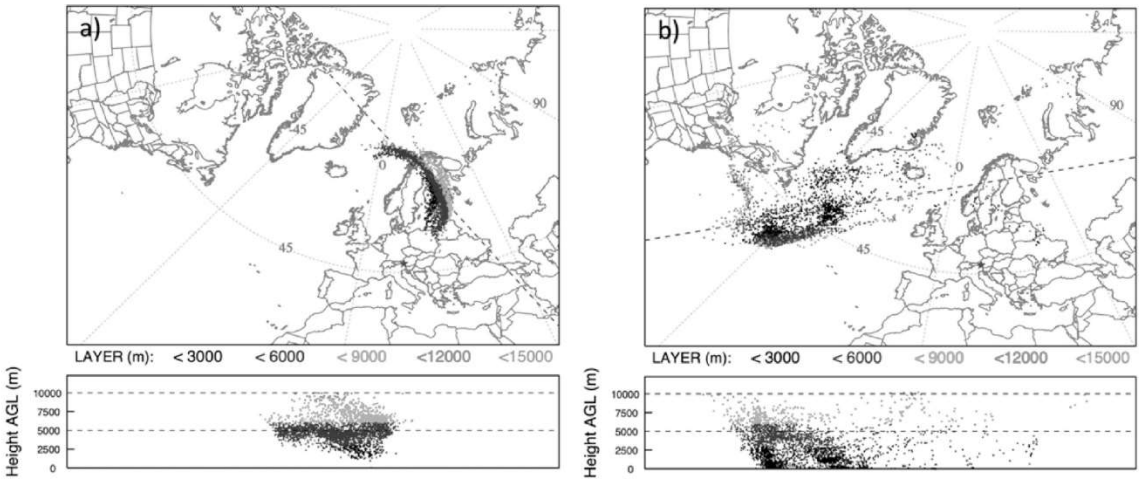

Fig. A.3. HYSPLIT backward dispersion model for 2017-02-15. a) Modelled dispersed particle position 48 h backwards in time indicating that most of the particles are at high-altitude – no surface contact, b) particle position 96 h backwards in time reaching the Atlantic Ocean surface, indicating possible marine sources.

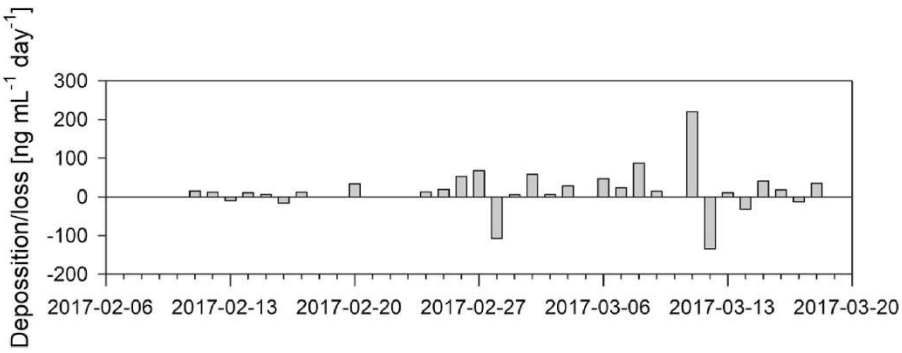

Fig. A.4. Deposition and loss of nanoplastics at/from the snow surface. Significant losses that happened 2017-02-28 and 2017-03-12 can be explained by meteorological condition favouring the concentration decrease – high wind and water condensation on the surface (e.g. frost). The observed losses suggest that our depositions and concentration values are indeed conservative, and possibly underestimated.

Appendix A. Supplementary data

Supplementary data to this article can be found online at https://doi.org/10.1016/j.envpol.2021.117697.

References

Allen, S., et al., 2019. Atmospheric transport and deposition of microplastics in a remote mountain catchment. Nat. Geosci. 1.

Allen, S., et al., 2020. Examination of the ocean as a source for atmospheric microplastics. PloS One 15, e0232746.

Apte, J.S., Marshall, J.D., Cohen, A.J., Brauer, M., 2015. Addressing global mortality from ambient PM2.5. Environ. Sci. Technol. 49, 8057–8066.

Bergmann, M., et al., 2019. White and wonderful? Microplastics prevail in snow from the Alps to the arctic. Sci. Adv. 5, eaax1157.

Brahney, J., Hallerud, M., Heim, E., Hahnenberger, M., Sukumaran, S., 2020. Plastic rain in protected areas of the United States. Science 368, 1257–1260.

Cappellin, L., et al., 2012. On quantitative determination of volatile organic compound concentrations using proton transfer reaction time-of-flight mass spectrometry. Environ. Sci. Technol. 46, 2283–2290.

da Costa, J.P., Santos, P.S.M., Duarte, A.C., Rocha-Santos, T., 2016. (Nano)plastics in the environment – sources, fates and effects. Sci. Total Environ. 566–567, 15–26.

Dris, R., Gasperi, J., Saad, M., Mirande, C., Tassin, B., 2016. Synthetic fibers in atmospheric fallout: a source of microplastics in the environment? Mar. Pollut. Bull. 104, 290–293.

Duan, B., Fairall, C.W., Thomson, D.W., 1988. Eddy correlation measurements of the dry deposition of particles in Wintertime. J. Appl. Meteorol. 27, 642–652.

Dubaish, F., Liebezeit, G., 2013. Suspended microplastics and black carbon particles in the Jade system, southern North sea. Water Air Soil Pollut. 224, 1352.

El Hadri, H., Gigault, J., Maxit, B., Grassl, B., Reynaud, S., 2020. Nanoplastic from mechanically degraded primary and secondary microplastics for environmental assessments. NanoImpact 17, 100206.

Els, N., Baumann-Stanzer, K., Larose, C., Vogel, T.M., Sattler, B., 2019. Beyond the Planetary Boundary Layer: Bacterial and Fungal Vertical Biogeography at Mount Sonnblick. Geo: Geography and Environment, Austria, e00069.

Evangeliou, N., et al., 2020. Atmospheric transport is a major pathway of microplastics to remote regions. Nat. Commun. 11, 3381.

Ferreira, I., Venâncio, C., Lopes, I., Oliveira, M., 2019. Nanoplastics and marine organisms: what has been studied? Environ. Toxicol. Pharmacol. 67, 1–7.

Gallagher, M.W., et al., 2002. Measurements and parameterizations of small aerosol deposition velocities to grassland, arable crops, and forest: influence of surface roughness length on deposition. J. Geophys. Res.: Atmos. 107. AAC 8-1-AAC 8-10.

Geyer, R., Jambeck, J.R., Law, K.L., 2017. Production, use, and fate of all plastics ever made. Sci. Adv. 3.

Holzinger, R., 2015. PTRwid: a new widget tool for processing PTR-TOF-MS data. Atmos. Meas. Tech. 8, 3903–3922.

Holzinger, R., Kasper-Giebl, A., Staudinger, M., Schauer, G., Röckmann, T., 2010. Analysis of the chemical composition of organic aerosol at the Mt. Sonnblick observatory using a novel high mass resolution thermal-desorption proton-transfer-reaction mass-spectrometer (hr-TD-PTR-MS). Atmos. Chem. Phys. 10, 10111–10128.

Holzinger, R., et al., 2019. Validity and limitations of simple reaction kinetics to calculate concentrations of organic compounds from ion counts in PTR-MS. Atmos. Meas. Tech. 12, 6193–6208.

Ivleva, N.P., Wiesheu, A.C., Niessner, R., 2017. Microplastic in aquatic ecosystems. Angew. Chem. Int. Ed. 56, 1720–1739.

Karl, T., et al., 2001. Variability-lifetime relationship of VOCs observed at the Sonnblick Observatory 1999—estimation of HO-densities. Atmos. Environ. 35, 5287–5300.

Kasper, A., Puxbaum, H., 1998. Seasonal variation of SO2, HNO3, NH3 and selected aerosol components at Sonnblick (3106ma.s.l.). Atmos. Environ. 32, 3925–3939.

Lehner, R., Weder, C., Petri-Fink, A., Rothen-Rutishauser, B., 2019. Emergence of nanoplastic in the environment and possible impact on human health. Environ. Sci. Technol. 53, 1748–1765.

Lindinger, W., Hansel, A., Jordan, A., 1998. On-line monitoring of volatile organic compounds at pptv levels by means of proton-transfer-reaction mass spectrometry (PTR-MS) medical applications, food control and environmental research. Int. J. Mass Spectrom. Ion Process. 173, 191–241.

Liu, K., et al., 2019. Consistent transport of terrestrial microplastics to the ocean through atmosphere. Environ. Sci. Technol. 53, 10612–10619.

Materić, D., Kasper-Giebl, A., Kau, D., Anten, M., Greilinger, M., Ludewig, E., van Sebille, E., Röckmann, T., Holzinger, R., 2020. Micro- and nanoplastics in alpine snow: a new method for chemical identification and (Semi)Quantification in the Nanogram range. Environ. Sci. Technol. 54, 2353–2359. https://doi.org/10.1021/acs.est.9b07540. Accessed 12 February 2020.

Materić, D., Ludewig, E., Xu, K., Röckmann, T., Holzinger, R., 2019. Brief communication: analysis of organic matter in surface snow by PTR-MS – implications for dry deposition dynamics in the Alps. Cryosphere 13, 297–307.

Materić, D., et al., 2017. Characterisation of the semi-volatile component of dissolved organic matter by thermal desorption – proton transfer reaction – mass spectrometry. Sci. Rep. 7, 15936.

Mintenig, S.M., Bäuerlein, P.S., Koelmans, A.A., Dekker, S.C., van Wezel, A.P., 2018. Closing the gap between small and smaller: towards a framework to analyse nano- and microplastics in aqueous environmental samples. Environ. Sci.: Nano 5, 1640–1649.

Napper, I.E., Thompson, R.C., 2019. Environmental deterioration of biodegradable, oxo-biodegradable, compostable, and conventional plastic carrier bags in the sea, soil, and open-air over a 3-year period. Environ. Sci. Technol. 53, 4775–4783.

Oberdörster, G., 1993. Lung dosimetry: pulmonary clearance of inhaled particles. Aerosol. Sci. Technol. 18, 279–289.

Oriekhova, O., Stoll, S., 2018. Heteroaggregation of nanoplastic particles in the presence of inorganic colloids and natural organic matter. Environ. Sci.: Nano 5, 792–799.

Peacock, M., Materić, D., Kothawala, D.N., Holzinger, R., Futter, M.N., 2018. Understanding dissolved organic matter reactivity and composition in lakes and streams using proton-transfer-reaction mass spectrometry (PTR-MS). Environ. Sci. Technol. Lett. 5, 739–744. https://doi.org/10.1021/acs.estlett.8b00529. Accessed 8 November 2018.

PlasticsEurope, 2019. Plastics - the Facts 2019 (July 6, 2020).

Pradel, A., et al., 2020. Deposition of environmentally relevant nanoplastic models in sand during transport experiments. Chemosphere 255, 126912.

Revel, M., Châtel, A., Mouneyrac, C., 2018. Micro(nano)plastics: a threat to human health? Curr. Opin. Environ. Sci. Health 1, 17–23.

Schwaferts, C., Niessner, R., Elsner, M., Ivleva, N.P., 2019. Methods for the analysis of submicrometer- and nanoplastic particles in the environment. Trac. Trends Anal. Chem. 112, 52–65.

Stapleton, P.A., 2019. Toxicological considerations of nano-sized plastics. AIMS Environ. Sci. 6, 367.

Stein, A.F., et al., 2015. NOAA's HYSPLIT atmospheric transport and dispersion modeling system. Bull. Am. Meteorol. Soc. 96, 2059–2077.

GEOSTAT, 2020. GEOSTAT - GISCO - Eurostat [WWW Document], n.d. GEOSTAT - Eurostat. https://ec.europa.eu/eurostat/web/gisco/geodata/reference-data/population-distribution-demography/geostat. accessed 7.12.21.

Ter Halle, A., et al., 2017. Nanoplastic in the North atlantic subtropical gyre. Environ. Sci. Technol. 51, 13689–13697.
Wright, S.L., Kelly, F.J., 2017. Plastic and human health: a micro issue? Environ. Sci. Technol. 51, 6634–6647.
Wright, S.L., Ulke, J., Font, A., Chan, K.L.A., Kelly, F.J., 2020. Atmospheric microplastic deposition in an urban environment and an evaluation of transport. Environ. Int. 136, 105411.